Comparative mapping of the TSC1 region of chromosome 9q34 in fugu rubripes using the human ATS-V gene. J. B. M ALI¹, M. CLARK², R. FURLONG¹ and A. J. GREEN^{1,3}. ¹Department of Pathology, University of Cambridge, UK; ²Molecular Genetics Unit, Department of Medicine, University of Cambridge, UK; ³Department of Medical Genetics, University of Cambridge, UK

The critical region for the TSC1 gene lies in a region of 2·7 MB between the markers D9S149 and D9S114 on chromosome 9q34. Physical mapping of this region has been hampered by the difficulty in constructing a physical map of the centromeric part of this area. To circumvent this problem, we are using the compact genome of Fugu rubripes to search for areas of conserved synteny with 9q34.

The Fugu rubripes genome is almost 8 times smaller than the human, and has far less repetitive DNA. There is strong conservation of gene sequence, the exon-intron structure is almost identical, and introns are considerably smaller than in man. Gene density is therefore much higher. There are already several known areas of conserved synteny between man and Fugu rubripes, with the TSC2 and PKD1 genes adjacent to each other in both species. We are therefore building a comparative map of 9q34 in the Fugu rubripes genome, using known conserved human genes. This may provide a resource of new genes at high density from an area that is difficult to clone in humans.

The ATSV (Axonal Transporter of Synaptic Vesicles) gene is a novel gene lying approximately 100 kb centromeric to the ABO locus on 9q34, which shows homology to the kinesin gene family in several species. We have used two approaches to find this gene in Fugu rubripes. We designed degenerate PCR primers to the conserved ATP-binding domain of the known kinesin genes, and used the Fugu rubripes genome as a template. Several closely related sequences were obtained which have strong homology to ATS-V and kinesin-related genes from other species. We used these sequences, as well as human ATS-V cDNA clones, to screen a Fugu rubripes genomic cosmid library. Secondary positive clones were subcloned, and sequenced. Subclones of one cosmid contained sequence with strong homology to the kinesin heavy chains and ATS-V. We are now sequencing further subclones of this cosmid at low stringency to find further coding sequence. Once characterised, this cosmid will be used to generate a physical map of Fugu rubripes, whose clones can be mapped back to the human genome.

Chromosome 9 loci in patients with defined outcome in transitional cell carcinoma of the urinary bladder: are there markers of disease progression and recurrence? J. M. S. BARTLETT¹, A. D. WATTERS¹, S. MARTIN¹, J. J. GOING², K. M. GRIGOR³ and T. G. COOKE¹. ¹ Glasgow University Department of Surgery, Glasgow Royal Infirmary, Glasgow, G31 2ER; ² Glasgow University Department of Pathology, Glasgow Royal Infirmary, G4 0SF, UK; ³ Edinburgh University Department of Pathology, Edinburgh, EH8 9AG, UK

This study demonstrates that loss of heterozygosity at chromosome 9 loci in patients with transitional cell carcinoma of the urinary bladder (TCC) may predict disease recurrence and progression and may affect survival.

To explore genetic events underlying the multistage natural history of transitional cell carcinoma of the urinary bladder (TCC) we have analysed tumours from three patient groups: (a) patients with superficial, non-recurrent TCC (NR) with at least 3 years disease-free follow up, (b) patients with

recurrent but non-progressive TCC (RNP) and (c) patients with recurrent progressive TCC (RP). 129 archival TCC of various grades and stages from 46 patients were evaluated for loss of heterozygosity (LOH) at markers spanning chromosome 9.

Loss of homozygosity occurred in 28% of samples showing some loss at CDKN2. There was some correlation between pathological grade and two of the markers but no relationship with tumour stage. LOH occurred rarely in non-malignant samples, mainly in dysplastic urothelium, and could precede morphological abnormality.

Investigation of TCC patients classified by recurrence and/or progression has demonstrated that loss of chromosome 9, as detected by FISH analysis of the pericentromeric alpha satellite marker at 9q12, occurs early.

Of 71 TCCs, in which multiple tumour areas were analysed, 69 tumours (97%) demonstrated the same chromosome 9 copy number in all areas (2–6) analysed; only two tumours demonstrated heterogeneity for this locus. Twenty-two TCCs were detected with consistent monosomic scores. Loss of chromosome 9 persisted in all subsequent TCC from patients who had lost this marker in their primary TCC. 30% (6/20) of patients with subsequent disease recurrence demonstrated loss of chromosome 9 in their primary and all subsequent TCC analysed. Patients (n=11) with non-recurrent TCC did not show loss of chromosome 9 in their TCC (p=0.047). Patients with primary TCC monosomic for chromosome 9 were more likely to die during the course of follow up (p=0.022). LOH occured significantly more frequently at D9S67 (9q34:3) & ABL (9q34:1) in TCC from patients with recurring, progressive disease. Whilst patient numbers are small this suggests that molecular markers, present in primary and subsequent tumours, may identify patients at greater risk of recurrence or progression.

It is proposed that loss of chromosome 9 loci from primary TCC of the urinary bladder indentified patients at high risk of recurrence and progression. A marker at 9q12 appears to predict disease recurrence, whilst a second marker at 9q34 appears to predict disease progression. Both lesions can be detected early in patients' disease process and may predict outcome in terms of survival.

Integrated radiation hybrid and YAC map of chromosome 9p. M. BOUZYK¹, S. P. BRYANT¹, C. EVANS¹, S. GUIOLI², S. FORD¹, B. LAGUDA¹, K. SCHMIDT², P. N. GOODFELLOW², R. EKONG³, S. ROUSSEAUX³ and N. K. SPURR¹. ¹ICRF Clare Hall Laboratories, South Mimms, Herts, UK; ²Department of Genetics, University of Cambridge, Cambridge, UK; ³MRC Human Biochemical Genetics Unit, University College, London, UK.

A radiation hybrid panel has been constructed for chromosome 9 using the somatic cell hybrid GM10611 as the paternal cell line fused to the hamster cell line a23. The hybrid GM10611 was characterised by FISH and reverse painting onto spreads of normal human metaphase chromosomes. It contains human chromosome 9 as the only cytogenetically detectable human material and it was irradiated with 6000 rads of X-rays prior to fusion. A total of 93 independent clones were isolated, frozen stocks and DNA were prepared from each clone. These clones have been screened using PCR amplification and oligonucleotide primers for STSs specific for 114 single copy loci mapping to the short arm of chromosome 9. The average retention frequency of these hybrids was approximately 20%. We have been able to construct a framework map containing 31 markers [TEL-D9S129-D9S54-D9S178-D9S132-D9S199-AFMa302ze1-RLN1-D9S281-D9S749-D9S144-D9S775-D9S168-D9S269-D9S1217-TYRP1-D9S267-D9S268-D9S274-D9S1211-TALIN-D9S156-D9S157-MLLT3-CDKN2-D9S171-D9S265-D9S270-D9S104-D9S319-D9S43-D9S304-CENT] ordered by analysing co-

retention patterns with support for the order greater than 1000:1 with an average physical distance of 1·7 Mb. In addition we have placed the remaining markers that could not be mapped to a single interval with this support, to a range of intervals on the framework map. Several genes assigned to 9p with a wide resolution were localised to a more precise interval on the radiation hybrid map. The STS oligonucleotide primers used in the construction of the radiation hybrid map have been used to isolate and order YACs assigned to 9p, identified from the CEPH mega-YAC library. 91 STS markers have screened positive with at least one YAC. A total of 88 individual YACs (with an average size of 1 Mb) have been placed on the map in a series of contigs and in some cases mapped cytogenetically by FISH. Additionally the YACs are currently being used to order approximately positioned markers on the original RH map, thereby reducing the physical distance between uniquely positioned markers on the integrated map.

LOH at 9p21 centromeric to CDKN2a in lung cancer. L. J. CAMPBELL¹, L. J. MEAD¹, M. T. GILLESPIE², K. C. RAYEROUX¹, U. RANE³ and L. B. IRVING⁴. ¹ Victorian Cancer Cytogenetics Service; ²St. Vincents Institute of Medical Research; ³ Cytology Department; ⁴St. Vincents Hospital, Fitzroy, Victoria, 3065 and Austin and Repatriation Medical Centre, Heidelberg, Victoria, 3081, Australia.

Cytogenetic deletions of 9p have been observed in many tumour types, including 79–83% of non-small cell lung cancers (NSCLC), prompting the search for tumour suppressor genes (TSG) in the region. The identification of the p16 gene (CDKN2a) within the region of loss on 9p21 appeared to identify a TSG of particular importance in a wide variety of tumours, based on the high proportion of cell lines exhibiting homozygous loss of CDKN2a. However, the percentage of fresh NSCLC tumours showing loss of CDKN2a has correlated poorly in several studies with the reported incidence of 9p loss as identified cytogenetically.

To investigate the possibility of a second TSG locus at 9p21, we have studied 32 paired normal lung and early stage primary lung tumours for loss of heterozygosity (LOH) in this region. Microdissection was used to obtain relatively pure samples of tumour cells and then PCR was performed directly on cell lysates, using primer pairs for 13 microsatellite markers spanning the region 9p12 to 9p23.

LOH at one or more markers was seen in 19 of the 32 tumour samples (59%). The marker D9S942, located within CDKN2a, showed 17% LOH whereas 52% of samples for which the marker D9S259 was informative exhibited LOH. A number of tumours showed complex patterns of loss with apparently more than one region of deletion within 9p. These findings suggest that another focus for deletions may exist within 9p21, centromeric to CDKN2a.

The isolation of transcribed sequences from the 9q22 region. B. P. CHADWICK, F. OBERMAYR, L. PATEL, A. WHITWORTH, K. HASENPUSCH-THEIL and A. M. FRISCHAUF. *Imperial Cancer Research Fund, London, WC2A 3PX. UK.*

We have used cDNA selection and EST fine mapping to identify transcribed sequences from the human 9q22 region. cDNA selection was carried out upon cosmid and PAC contigs positive for markers from the 9q22 region. ESTs from 9q were PCR fine mapped upon a set of 109 radiation

hybrids with well defined breaks in 9q22. The combined techniques resulted in the identification of 20 cDNA groups including the known genes XPA, FACC, FBP, TMOD and ABC1. Physical mapping of the 9q22 region has included pulsed field gel mapping and the construction of cosmid and PAC contigs for the region. Approximately 2 Mb are covered in PAC and cosmid contigs which are being restriction analysed for minimal coverage.

Refining the chromosome 9 integrated map. A. COLLINS and N. E. MORTON.

Efforts to refine the integrated map of chromosome 9 have concentrated on enhancements to software in the MAP+/ldb+ suite of programs and acquisition of location data from Internet and literature sources. The integrated map of chromosome 9 is now amongst the most complete available from our WWW site at http://cedar.genetics.soton.ac.uk/public_html. Included in the database and summary map are 325 loci mapped using MAP+ with data from the CEPH version 8 release. Of these, 182 loci are also in the recent GENETHON map with which there are a small number of local order discrepancies, mostly involving inversions of adjacent loci. Map lengths for the MAP+ map are 139·8 cM (standard error 9·7 cM) for the male map and 183·0 cM (standard error 10·5 cM) for the female map. The Rao mapping parameter P is estimated at 0·21 with a typing error frequency of E = 0·003. The summary map of chromosome 9 gives locations for more than 800 loci with physical, radiation hybrid, genetic or cytogenetic location data.

The location database will be further developed and updated in parallel with the Genome Interactive Database (GID) CD-ROM which includes CEPH, GENETHON, GENATLAS, ldb and comparative databases.

Present translocation grids for chromosome 9. J. L. DICKS, and T. HOURIHAN.

The aim of the poster is to present translocation grids for chromosome 9 produced using ACEDB software. The grids represent the reciprocal translocations involving chromosome 9 which have been identified in UK laboratories and submitted to the Chromosome Abnormality Database. They will be produced for both acquired and constitutional abnormalities. The grids will demonstrate that distribution of breakpoints is not random, and it is intended that they can be used to identify areas of interest to gene mappers and those studying the deleterious effects of chromosomal disruption. Grids were previously presented for chromosome 14 at the Single Chromosome Workshop, Chromosome 14 at Oxford in 1994.

The organisation and conservation of the human surfeit locus. T. R. DUHIG, O. MOR, C. MAGOULAS, J. GILLEY, N. ARMES, M. READ and M. FRIED. Eukaryotic Gene Organisation and Expression Laboratory, Imperial Cancer Research Fund, P.O. Box 123, Lincoln's Inn Fields, London WC2A 3PX, UK.

The Surfeit locus contains at least six tightly clustered housekeeping genes (Surf-1 to -6) with novel features. In contrast to the tens to hundreds of kilobases found between most adjacent mammalian genes only a small region separates any two adjacent Surfeit genes. The organization of the Surfeit

locus and the juxtaposition of the Surfeit genes is conserved between mouse, human and chicken (600 million years of divergent evolution) indicating that the Surfeit locus gene organisation may have biological significance. The Surfeit Locus genes are highly conserved and their linkage has been determined in a number of lower organisms. The human Surfeit locus has been mapped to 9q34·1 within the candidate region for TSC1. Preliminary SSCP analysis of some of the Surfeit genes has not revealed any differences associated with TSC1. Using cosmid, P1 and PAC clones we have constructed a contig around the human Surfeit Locus genes which contains part of the ABO glycosyltransferase gene. We have determined the orientation of the Surfeit Locus genes relative to the ABO Locus, the centromere and the telomere of 9q.

Comparative mapping chromosome 9. J. H. EDWARDS, J. PETERS, R. SELLEY, J. J. DICKS and A. G. SEARLE. *Medical Research Council Mammalian Genetics Unit, Harwell, Didcot, Oxon.*

The following data were abstracted in March 1996 and will be extended in August. Only loci for which acceptable homologies have been defined in man amd mouse are presented. The data from the rat, pig and sheep are from files maintained on the WWW, http://www.hgmp.mrc.ac.uk/

Rat http://ratmap.gen.gu.se/

Pig http://www.ri.bbsrc.ac.uk/teagdb.html

Sheep http://dirk.invermay.cri.nz

Those from from the cow have been assembled by Dr B. Rendse in Brisbane.

The October 1995 version is available at http://www.hgmp.mrc.ac.uk and later versions should shortly be available through both the Medical Research Council's Human Genome Resource Centre (HGRP) and from Harwell http://www.har.mrc.ac.uk

These will also be presented as diagrams and displayed in the ACEDB program and also include the subset of the full three generation CEPH familes related to these loci. The first number is an internal reference number. An * refers to an in situ localization.

Human	Mouse	Human	Mouse	Rat	Pig	Cow	Sheep
804 VLDLR	Vldlr	9 p24	19 B–D1				
805 JAK2	Jak2	9 p24	19 B–D2				
806 SLC1A1	Slc1a1	9 p24	19 B–D1				
$809 \mathrm{SNF}2\mathrm{L}2$	Snf212	$9 \mathrm{p}24 - \mathrm{p}23$	19 B–D1				
$813~\mathrm{AK3}$	Ak3	9 p24-p13	4 C7				
815 IFNB1	Ifb	9 p22	4 C3–C6*	5 q31-33	q15		
816 IFN1	Ifa	9 p21	4 C2-C6*	-	-		
817 CD72	Cd72	9 p	4 A1 - A5				
818 TEK	Tek	9 p21	4 C7				
$819 \mathrm{GGTB2}$	Ggtb	$9\mathrm{p}13$	4 A1-A5				2
$820~\mathrm{RMRP}$	Rmrp	9 p21-p12	4 p21-p12				
823 PAX5	Pax5	$9\mathrm{p}13$	$4\ \mathrm{A}1\mathrm{-A}5$				
824 CNTFR	Cntfr	$9 \mathrm{~p13}$	4 A1-A5				
825 ALDH5	Aldh5	$9 \mathrm{~p13}$	$11 \; A2 - B1$	5			
$831~\mathrm{GALT}$	Galt	9 p13	4 A1-A5				
833 ACO1	Aco1	9 p22-q32	4 A1-A5	5			
834 ANX1	$_{ m Lpc1}$	9 q11 - q22	$19 \mathrm{\ B-D1}$				
838 ALDH1	Aldh1	9 q21·1	19 B–D1	13			
839 PCSK5	Pesk5	$9~\mathrm{ptr-qtr}$	19 B–D1				
840 IREB1	Irebp	$9~\mathrm{ptr-qtr}$	4 A1-A5				
842 GCNT1	Gent1	$9 ext{ q}21$	13 A2–C1				

843 GAS1 Gas1 9 q21:3-q22 13 C1* 844 NTRK2 Ntrk2 9 q22:1-q22:2 13 A2-B3 848 SYK Syk 9 q22 13 Q22 849 TMOD Tmod 9 q22 4 A1-A5 850 FPGS Fpgs 9 q 2 B 3 850 FPGS Fpgs 9 q 2 B 3 852 FACC Face 9 q22:3-q32 13 B-C1 17 855 ALDOB Aldo2 9 q21:3-q22 4 A1-A5 5 856 ALAD Lv 9 q32-q34 4 A5-C2 8 857 C8G C8g 9 q22-3-q32 2 Cen-A2 8 859 TXN Txn 9 q32 4 A5-C2 8 865 HXB Tnc 9 q31-q32 4 A5-C1 8 865 HXB Tnc 9 q32-q34 4 A5-C2 1 866 PTGS1 Ptgs1 9 q32-q33 2 D* 3 867 AMBP Ambp 9 q32-q33 4 CI-C4 870 FTZF1 Ftzf1 9 q33 2 C1-D 870 EST Ftzf1 9 q33 2 C1-D	Human	Mouse	Human	Mouse	Rat	Pig	Cow	Sheep
844 NTRK2	843 GAS1	Gas1	9 q21.3-q22	13 C1*				
847 CTSL Ctsl 9 q22-1-q22-2 13 A2-B3 848 SYK Syk 9 q22 13 q22 849 TMOD Tmod 9 q22 4 A1-A5 850 FPGS Fpgs 9 q 2 B 3 3 3 852 FACC Face 9 q22-3 13 B-C1 17 855 ALDOB Aldo2 9 q21-3-q22 4 A1-A5 5 2 856 ALAD Lv 9 q32-q34 4 A5-C2 857 C8G C8g 9 q22-3-q32 2 Cen-A2 859 TXN Txn 9 q32 4 A1-A5 862 TAL2 Tal2 9 q31-q32 4 A5-C2 865 HXB Tne 9 q32-q34 4 A5-C2 1 866 PTGS1 Ptgs1 9 q32-q33 2 D* 3 867 AMBP Ambp 9 q32-q33 4 A5-C2 868 PAPPA Pappa 9 q33-1 4 C1-C4 870 FTZF1 Ftzf1 9 q33 2 C1-D 873 GSN Gsn 9 q33 2 C1-D 873 GSN Gsn 9 q34-qter 2 C1-D 880 SPTAN1 Spna2 9 q34-1 2 B 882 EPB72 Epb7-2 9 q34-1 2 B 887 GCTA1 Ggta1 9 q33-q34 2 D-1 886 RPL7A Rpl7 9 q34-q34 2 B-1 889 LCN2 Len2 9 q34 2 B-1 890 PTGDS Ptgds 9 q34-2-q3+3 2 B-D	844 NTRK2							
848 SYK		Ctsl	$9 q^{2} 2 \cdot 1 - q^{2} 2 \cdot 2$					
849 TMOD	$848 \mathrm{SYK}$	Svk		13 q22				
850 FPGS Fpgs 9 q 2 B 3 852 FACC Face 9 q22·3 13 B-C1 17 855 ALDOB Aldo2 9 q21·3-q22 4 A1-A5 5 2 856 ALAD Lv 9 q32-q34 4 A5-C2 8 857 C8G C8g 9 q22·3-q32 2 Cen-A2 857 TXN Txn 9 q32 4 A1-A5 8 862 TAL2 Tal2 9 q31-q32 4 A5-C1 866 PTGS1 Ptgs1 9 q32-q33 2 D* 3 867 PTGS1 Ptgs1 9 q32-q33 2 D* 3 867 PTGS1 Ptgs1 9 q32-q33 4 A5-C2 1 868 PAPA Ambp 9 q32-q33 4 A5-C2 1 868 PTGS1 Ptgs1 9 q33-q33 2 C1-D 874 AK1 84 C1-C4 870 FTGS1 Ptgs1 9 q34-q4-q4 2 C1-D 874 AK1 871 FTGS1 9 q34-q4-q4 2 B <t< td=""><td>849 TMOD</td><td></td><td>1</td><td></td><td></td><td></td><td></td><td></td></t<>	849 TMOD		1					
852 FACC Face 9 q22·3 13 B-C1 17 855 ALDOB Aldo2 9 q21·3-q22 4 AI-A5 5 2 856 ALAD Lv 9 q32-q34 4 A5-C2 8 8 857 C8G C8g 9 q22·3-q32 2 Cen-A2 8 857 TXN Txn 9 q32 4 A1-A5 8 862 TAL2 Tal2 9 q31-q32 4 A5-C1 8 865 HXB Tne 9 q32-q34 4 A5-C2 1 866 PTG81 Ptgs1 9 q32-q33 4 A5-C2 1 866 PTG81 Ptgs1 9 q32-q33 4 A5-C2 1 867 AMBP Ambp 9 q32-q33 4 A5-C2 1 868 PAPPA Pappa 9 q33-q33 2 C1 868 PAPPA Pappa 9 q33-q33 2 C1-C4 874 AK1 876 FTZF1 Ftzf1 9 q33 2 C1-D 2 874 AK1 Ak1 9 q34-q1 2 B 3 3 3 876 ENG Eng 9 q34-qter 2 C1-D 880 EPTAN1 Spna2 9 q34-qter 2 C1-D 885 EPB72 Epb7-2 9 q34-1 2 B 886 RPL7A Rpl7 9 q33-q34 2 C1-D 896 AR7 887 BAS	$850 \; \mathrm{FPGS}$	Fpgs		$2~\mathrm{B}$	3			3
855 ALDOB Aldo2 9 q21·3-q22 4 A1-A5 5 2 856 ALAD Lv 9 q32-q34 4 A5-C2 8 857 C8G C8g 9 q22·3-q32 2 Cen-A2 8 859 TXN Txn 9 q32-q32 2 Cen-A2 8 859 TXN Txn 9 q31-q32 4 A5-C1 8 862 TAL2 Tal2 9 q31-q32 4 A5-C1 8 865 HXB Tne 9 q32-q33 2 D* 3 866 PTGS1 Ptgs1 9 q32-q33 2 D* 3 867 AMBP Ambp 9 q32-q33 4 A5-C2 1 868 PAPPA Pappa 9 q33 2 C1 4 A5-C2 870 FTZF1 Ftzf1 9 q33 2 C1-D4 8 870 FTZF1 Ftzf1 9 q33 2 C1-D 2 873 GSN Gsn 9 q33 2 C1-D 2 874 AK1 Ak1 9 q34-qter 2 C1-D 2 880 SPTAN1 Spna2 9 q34-1 2 B 2 882 EPB72 Epb7·2 9 q34-1 2 C1-D 8	$852 \; \mathrm{FACC}$			13 B–C1	17			
857 C8G C8g 9 q22·3-q32 2 Cen-A2 859 TXN Txn 9 q32 4 A1-A5 862 TAL2 Tal2 9 q31-q32 4 A5-C1 865 HXB Tne 9 q32-q34 4 A5-C2 1 866 PTGS1 Ptgs1 9 q32-q33·3 2 D* 3 867 AMBP Ambp 9 q32-q33 4 A5-C2 8 868 PAPPA Pappa 9 q33·1 4 C1-C4 8 870 FTZF1 Ftxf1 9 q33 2 C1-D 8 873 GSN Gsn 9 q33 2 C1-D 2 874 AK1 Ak1 9 q34·1 2 B 3 876 ENG Eng 9 q34·1 2 B 3 880 SPTAN1 Spna2 9 q34·1 2 B 8 882 EPB72 Epb7·2 9 q34·1 2 B 8 885 GGTA1 Ggta1 9 q33-q34 2 C1-D 8 886 RPL7A Rpl7 9 q33-q34 2 C1-D 8 887 PBX3 Pbx3 9 q34·1 2 B 8 891 ABL1 Abl 9 q34 <	855 ALDOB	Aldo2		4 A1 - A5	5			2
857 C8G C8g 9 q22·3-q32 2 Cen-A2 859 TXN Txn 9 q32 4 A1-A5 862 TAL2 Tal2 9 q31-q32 4 A5-C1 865 HXB Tnc 9 q32-q34 4 A5-C2 1 866 PTGS1 Ptgs1 9 q32-q33·3 2 D* 3 867 AMBP Ambp 9 q32-q33 4 A5-C2 8 868 PAPPA Pappa 9 q33·1 4 C1-C4 8 870 FTZF1 Ftxf1 9 q33 2 C1-D 8 872 C5 He 9 q33 2 C1-D 2 873 GSN Gsn 9 q33 2 C1-D 2 874 AK1 Ak1 9 q34·1 2 B 3 880 SPTAN1 Spna2 9 q34·1 2 B 8 882 EPB72 Epb7·2 9 q34·1 2 B 8 885 GGTA1 Ggta1 9 q33-q34 2 C1-D 2 886 RPL7A Rpl7 9 q33-q34 2 C1-D 8 887 PBX3 Pbx3 9 q34·1 2 B 8 891 ABL1 Abl 9 q34 <t< td=""><td>856 ALAD</td><td>Lv</td><td></td><td>4 A5 - C2</td><td></td><td></td><td></td><td></td></t<>	856 ALAD	Lv		4 A5 - C2				
859 TXN Txn 9 q32 4 A1-A5 862 TAL2 Tal2 9 q31-q32 4 A5-C1 865 HXB Tne 9 q32-q34 4 A5-C2 1 866 PTGS1 Ptgs1 9 q32-q33 2 D* 3 867 AMBP Ambp 9 q32-q33 4 A5-C2 4 868 PAPPA Pappa 9 q33 2 C1 4 870 FTZF1 Ftzf1 9 q33 2 C1-D 2 873 GSN Gsn 9 q33 2 C1-D 2 874 AK1 Ak1 9 q34·1 2 B 3 876 ENG Eng 9 q34-qter 2 C1-D 2 880 SPTAN1 Spna2 9 q34·1 2 B 3 882 EPB72 Epb7·2 9 q34·1 2 C1-D 2 885 GGTA1 Ggta1 9 q33-q34 2 D 1 886 RPL7A Rpl7 9 q33-q34 2 C1-D 2 887 PBX3 Pbx3 9 q34-q3 2 C1-D 2 887 PBX3 Pbx3 9 q34-1 2 B 3 4 890 ASS Ass1 <td>$857~\mathrm{C8G}$</td> <td>C8g</td> <td></td> <td>2 Cen-A2</td> <td></td> <td></td> <td></td> <td></td>	$857~\mathrm{C8G}$	C8g		2 Cen-A2				
862 TAL2 Tal2 9 q31-q32 4 A5-C1 865 HXB The 9 q32-q34 4 A5-C2 1 866 PTGS1 Ptgs1 9 q32-q33·3 2 D* 3 867 AMBP Ambp 9 q32-q33 4 A5-C2 8 868 PAPPA Pappa 9 q33 2 C1 8 870 FTZF1 Ftzf1 9 q33 2 C1-D 8 873 GSN Gsn 9 q33 2 C1-D 2 874 AK1 Ak1 9 q34·1 2 B 3 876 ENG Eng 9 q34-qter 2 C1-D 8 880 SPTAN1 Spna2 9 q34·1 2 B 3 882 EPB72 Epb7·2 9 q34·1 2 C1-D 8 885 GGTA1 Ggta1 9 q33-q34 2 D 1 886 RPL7A Rpl7 9 q33-q34 2 C1-D 8 887 PBX3 Pbx3 9 q34-q34 2 C1-D 8 890 ASS Ass1 9 q34-1 2 B 8 891 ABLI Abl 9 q34 2 B 3 q12 892 VAV2 Vav2	859 TXN			4 A1 - A5				
866 PTGS1 Ptgs1 9 q32-q33·3 2 D* 3 867 AMBP Ambp 9 q32-q33 4 A5-C2 868 PAPPA Pappa 9 q33·1 4 C1-C4 870 FTZF1 Ftzf1 9 q33 2 C1 872 C5 He 9 q33 2 C1-D 873 GSN Gsn 9 q34·1 2 B 874 AK1 Ak1 9 q34·1 2 B 880 SPTAN1 Spna2 9 q34·1 2 B 880 SPTAN1 Spna2 9 q34·1 2 C1-D 885 GGTA1 Ggta1 9 q33-q34 2 D 1 886 RPL7A Rpl7 9 q33-q34 2 C1-D 886 RPL7A 890 ASS Ass1 9 q34·1 2 B 890 ASS Ass1 9 q34·1 2 B 891 ABL1 Abl 9 q34·1 2 B 891 ABL1 Abl 9 q34 2 B 3 q12 892 VAV2 Vav2 9 q34 2 B 894 RXRA Rxra 9 q34·2 2 B 896 DBH Dbh 9 q34·2-q34·3 2 B 899 PTGDS Ptgds 9 q34·2-q	$862~\mathrm{TAL2}$	Tal2		4 A5–C1				
867 AMBP Ambp 9 q32-q33 4 A5-C2 868 PAPPA Pappa 9 q33·1 4 C1-C4 870 FTZF1 Ftzf1 9 q33 2 C1 872 C5 He 9 q33 2 C1-D 873 GSN Gsn 9 q33 2 C1-D 874 AK1 Ak1 9 q34·1 2 B 876 ENG Eng 9 q34-qter 2 C1-D 880 SPTAN1 Spna2 9 q34·1 2 B 882 EPB72 Epb7·2 9 q34·1 2 C1-D 885 GGTA1 Ggta1 9 q33-q34 2 D 1 886 RPL7A Rpl7 9 q33-q34 2 C1-D 887 PBX3 Pbx3 9 q34-q34 2 C1-D 890 ASS Ass1 9 q34·1 2 B 891 ABL1 Abl 9 q34 2 B* 893 LCN2 Vav2 9 q34 2 B 894 RXRA Rxra 9 q34 2 B 896 DBH Dbh 9 q34·2-q34·3 2 B 898 PAEP Paep 9 q34 2 F1-F3 899 PTGDS Ptgds 9 q34·2-q34·3 <td< td=""><td>$865~\mathrm{HXB}$</td><td>Tne</td><td>9 q32 - q34</td><td>4 A5 - C2</td><td></td><td>1</td><td></td><td></td></td<>	$865~\mathrm{HXB}$	Tne	9 q32 - q34	4 A5 - C2		1		
868 PAPPA Pappa 9 q33·1 4 C1-C4 870 FTZF1 Ftzf1 9 q33 2 C1 872 C5 Hc 9 q33 2 C1-D 873 GSN Gsn 9 q33 2 C1-D 874 AK1 Ak1 9 q34·1 2 B 876 ENG Eng 9 q34-qter 2 C1-D 880 SPTAN1 Spna2 9 q34·1 2 B 882 EPB72 Epb7·2 9 q34·1 2 C1-D 885 GGTA1 Ggta1 9 q33-q34 2 D 1 886 RPL7A Rpl7 9 q33-q34 2 C1-D 887 PBX3 Pbx3 9 q33-q34 2 C1-D 890 ASS Ass1 9 q34·1 2 B 891 ABL1 Abl 9 q34 2 B 891 ABL1 Abl 9 q34 2 B 893 LCN2 Lcn2 9 q34 2 B 894 RXRA Rxra 9 q34 2 B 896 DBH Dbh 9 q34·2-q34·3 2 B 898 PAEP Paep 9 q34 2 F1-F3 899 PTGDS Ptgds 9 q34·2-q34·3 2 B-D <td>866 PTGS1</td> <td>Ptgs1</td> <td>$9 q32-q33\cdot 3$</td> <td>2 D*</td> <td>3</td> <td></td> <td></td> <td></td>	866 PTGS1	Ptgs1	$9 q32-q33\cdot 3$	2 D*	3			
$\begin{array}{cccccccccccccccccccccccccccccccccccc$	867 AMBP	Ambp	9 q32-q33	4 A5 - C2				
$\begin{array}{cccccccccccccccccccccccccccccccccccc$	868 PAPPA	Pappa	9 q33·1	4 C1-C4				
873 GSN Gsn 9 q33 2 C1-D 2 874 AK1 Ak1 9 q34·1 2 B 3 876 ENG Eng 9 q34-qter 2 C1-D 880 SPTAN1 Spna2 9 q34·1 2 B 882 EPB72 Epb7·2 9 q34·1 2 C1-D 885 GGTA1 Ggta1 9 q33-q34 2 D 1 886 RPL7A Rpl7 9 q33-q34 2 C1-D 887 PBX3 Pbx3 9 q33-q34 2 C1-D 890 ASS Ass1 9 q34·1 2 B 891 ABL1 Abl 9 q34 2 B* 892 VAV2 Vav2 9 q34 2 B 893 LCN2 Lcn2 9 q34 2 B 894 RXRA Rxra 9 q34·3 2 B 896 DBH Dbh 9 q34·2-q34·3 2 A2-B* 898 PAEP Paep 9 q34 2 F1-F3 899 PTGDS Ptgds 9 q34·2-q34·3 2 B-D	870 FTZF1	Ftzf1		2 C1				
874 AK1 Ak1 9 q34·1 2 B 3 876 ENG Eng 9 q34-qter 2 C1-D 880 SPTAN1 Spna2 9 q34·1 2 B 882 EPB72 Epb7·2 9 q34·1 2 C1-D 885 GGTA1 Ggta1 9 q33-q34 2 D 1 886 RPL7A Rpl7 9 q33-q34 2 A2-B 887 PBX3 Pbx3 9 q33-q34 2 C1-D 890 ASS Ass1 9 q34·1 2 B 891 ABL1 Abl 9 q34 2 B* 892 VAV2 Vav2 9 q34 2 B 893 LCN2 Len2 9 q34 2 D 894 RXRA Rxra 9 q34·2 2 B 896 DBH Dbh 9 q34·3 2 B 897 COL5A1 Col5a1 9 q34·2-q34·3 2 A2-B* 898 PAEP Paep 9 q34 2 F1-F3 899 PTGDS Ptgds 9 q34·2-q34·3 2 B-D	872 C5	$_{\mathrm{He}}$	$9 ext{ q}33$	2 C1-D				
876 ENG Eng 9 q34-qter 2 C1-D 880 SPTAN1 Spna2 9 q34·1 2 B 882 EPB72 Epb7·2 9 q34·1 2 C1-D 885 GGTA1 Ggta1 9 q33-q34 2 D 1 886 RPL7A Rpl7 9 q33-q34 2 A2-B 887 PBX3 Pbx3 9 q33-q34 2 C1-D 890 ASS Ass1 9 q34·1 2 B 891 ABL1 Abl 9 q34 2 B* 892 VAV2 Vav2 9 q34 2 B 893 LCN2 Lcn2 9 q34 2 D 894 RXRA Rxra 9 q34·2 2 B 896 DBH Dbh 9 q34·2-q34·3 2 B 897 COL5A1 Col5a1 9 q34·2-q34·3 2 A2-B* 898 PAEP Paep 9 q34 2 F1-F3 899 PTGDS Ptgds 9 q34·2-q34·3 2 B-D	$873 \mathrm{GSN}$	Gsn	$9 ext{ q}33$	2 C1-D				2
880 SPTAN1 Spna2 9 q34·1 2 B 882 EPB72 Epb7·2 9 q34·1 2 C1-D 885 GGTA1 Ggta1 9 q33-q34 2 D 1 886 RPL7A Rpl7 9 q33-q34 2 A2-B 887 PBX3 Pbx3 9 q33-q34 2 C1-D 890 ASS Ass1 9 q34·1 2 B 891 ABL1 Abl 9 q34 2 B* 892 VAV2 Vav2 9 q34 2 B 893 LCN2 Lcn2 9 q34 2 D 894 RXRA Rxra 9 q34·2 2 B 896 DBH Dbh 9 q34·3 2 B 897 COL5A1 Col5a1 9 q34·2-q34·3 2 A2-B* 898 PAEP Paep 9 q34 2 F1-F3 899 PTGDS Ptgds 9 q34·2-q34·3 2 B-D	874 AK1	Ak1	9 q34·1	2 B	3			3
882 EPB72 Epb7·2 9 q34·1 2 C1-D 885 GGTA1 Ggta1 9 q33-q34 2 D 1 886 RPL7A Rpl7 9 q33-q34 2 A2-B 887 PBX3 Pbx3 9 q33-q34 2 C1-D 890 ASS Ass1 9 q34·1 2 B 891 ABL1 Abl 9 q34 2 B* 3 q12 892 VAV2 Vav2 9 q34 2 B 893 LCN2 Lcn2 9 q34 2 D 894 RXRA Rxra 9 q34 2 B 896 DBH Dbh 9 q34·3 2 B 897 COL5A1 Col5a1 9 q34·2-q34·3 2 A2-B* 898 PAEP Paep 9 q34 2 F1-F3 899 PTGDS Ptgds 9 q34·2-q34·3 2 B-D	$876 \; \mathrm{ENG}$	Eng	$9 ext{ q34-qter}$	2 C1-D				
885 GGTA1 Ggta1 9 q33-q34 2 D 1 886 RPL7A Rpl7 9 q33-q34 2 A2-B 887 PBX3 Pbx3 9 q33-q34 2 C1-D 890 ASS Ass1 9 q34·1 2 B 891 ABL1 Abl 9 q34 2 B* 3 q12 892 VAV2 Vav2 9 q34 2 B 893 LCN2 Lcn2 9 q34 2 D 894 RXRA Rxra 9 q34 2 B 896 DBH Dbh 9 q34·3 2 B 897 COL5A1 Col5a1 9 q34·2-q34·3 2 A2-B* 898 PAEP Paep 9 q34 2 F1-F3 899 PTGDS Ptgds 9 q34·2-q34·3 2 B-D	880 SPTAN1	Spna2	9 q34·1	2 B				
886 RPL7A Rpl7 9 q33-q34 2 A2-B 887 PBX3 Pbx3 9 q33-q34 2 C1-D 890 ASS Ass1 9 q34·1 2 B 891 ABL1 Abl 9 q34 2 B* 3 q12 892 VAV2 Vav2 9 q34 2 B 893 LCN2 Lcn2 9 q34 2 D 894 RXRA Rxra 9 q34 2 B 896 DBH Dbh 9 q34·3 2 B 897 COL5A1 Col5a1 9 q34·2-q34·3 2 A2-B* 898 PAEP Paep 9 q34 2 F1-F3 899 PTGDS Ptgds 9 q34·2-q34·3 2 B-D	882 EPB72	$Epb7\cdot2$	9 q34·1	2 C1-D				
887 PBX3 Pbx3 9 q33-q34 2 C1-D 890 ASS Ass1 9 q34·1 2 B 891 ABL1 Abl 9 q34 2 B* 3 q12 892 VAV2 Vav2 9 q34 2 B 893 LCN2 Lcn2 9 q34 2 D 894 RXRA Rxra 9 q34 2 B 896 DBH Dbh 9 q34·3 2 B 897 COL5A1 Col5a1 9 q34·2-q34·3 2 A2-B* 898 PAEP Paep 9 q34 2 F1-F3 899 PTGDS Ptgds 9 q34·2-q34·3 2 B-D	$885 \mathrm{GGTA1}$	Ggta1	9 q33 - q34	2 D		1		
890 ASS Ass1 9 q34·1 2 B 891 ABL1 Abl 9 q34 2 B* 3 q12 892 VAV2 Vav2 9 q34 2 B 893 LCN2 Lcn2 9 q34 2 D 894 RXRA Rxra 9 q34 2 B 896 DBH Dbh 9 q34·3 2 B 897 COL5A1 Col5a1 9 q34·2-q34·3 2 A2-B* 898 PAEP Paep 9 q34 2 F1-F3 899 PTGDS Ptgds 9 q34·2-q34·3 2 B-D	886 RPL7A	Rpl7	9 q33-q34	2 A2-B				
891 ABL1 Abl 9 q34 2 B* 3 q12 892 VAV2 Vav2 9 q34 2 B 893 LCN2 Lcn2 9 q34 2 D 894 RXRA Rxra 9 q34 2 B 896 DBH Dbh 9 q34·3 2 B 897 COL5A1 Col5a1 9 q34·2-q34·3 2 A2-B* 898 PAEP Paep 9 q34 2 F1-F3 899 PTGDS Ptgds 9 q34·2-q34·3 2 B-D	887 PBX3	Pbx3	9 q33-q34	2 C1-D				
892 VAV2 Vav2 9 q34 2 B 893 LCN2 Lcn2 9 q34 2 D 894 RXRA Rxra 9 q34 2 B 896 DBH Dbh 9 q34·3 2 B 897 COL5A1 Col5a1 9 q34·2-q34·3 2 A2-B* 898 PAEP Paep 9 q34 2 F1-F3 899 PTGDS Ptgds 9 q34·2-q34·3 2 B-D	890 ASS	Ass1	9 q34·1	$2 \mathrm{~B}$				
893 LCN2 Lcn2 9 q34 2 D 894 RXRA Rxra 9 q34 2 B 896 DBH Dbh 9 q34·3 2 B 897 COL5A1 Col5a1 9 q34·2-q34·3 2 A2-B* 898 PAEP Paep 9 q34 2 F1-F3 899 PTGDS Ptgds 9 q34·2-q34·3 2 B-D	891 ABL1	Abl	9 q34	$2 B^*$	3 q 12			
894 RXRA Rxra 9 q34 2 B 896 DBH Dbh 9 q34·3 2 B 897 COL5A1 Col5a1 9 q34·2-q34·3 2 A2-B* 898 PAEP Paep 9 q34 2 F1-F3 899 PTGDS Ptgds 9 q34·2-q34·3 2 B-D	892 VAV2	Vav2	$9 ext{ q}34$	$2~\mathrm{B}$				
896 DBH Dbh 9 q34·3 2 B 897 COL5A1 Col5a1 9 q34·2-q34·3 2 A2-B* 898 PAEP Paep 9 q34 2 F1-F3 899 PTGDS Ptgds 9 q34·2-q34·3 2 B-D	893 LCN2	Len2	9 q34	2 D				
897 COL5A1 Col5a1 9 q34·2-q34·3 2 A2-B* 898 PAEP Paep 9 q34 2 F1-F3 899 PTGDS Ptgds 9 q34·2-q34·3 2 B-D	894 RXRA	Rxra	$9 ext{ q}34$	$2~\mathrm{B}$				
898 PAEP Paep 9 q34 2 F1-F3 899 PTGDS Ptgds 9 q34·2-q34·3 2 B-D	896 DBH	Dbh	9 q34·3	$2~\mathrm{B}$				
899 PTGDS Ptgds 9 q34·2-q34·3 2 B-D	897 COL5A1	Col5a1	$9 q34 \cdot 2 - q34 \cdot 3$	2 A2-B*				
	898 PAEP	Paep	9 q34	2 F1-F3				
004 CTT	899 PTGDS	Ptgds		2 B-D				
901 CEL Cel 9 q34·3 2 B	901 CEL	Cel	9 q34.3	$2~\mathrm{B}$				
903 NOTCH1 Notch1 9 q34·3 2 B	903 NOTCH1	Notch1		2 B				

Towards the identification of a 9p linked gene involved in human sex determination. S. GUIOLI¹, K. SCHMITT^{1,2}, M. BOUZYK³, N. K. SPURR³ and P. N. GOODFELLOW¹. ¹Department of Genetics, University of Cambridge, UK; ²Millenium Pharmaceuticals Inc., Cambridge, MA, USA; ³Imperial Cancer Research Fund, London, UK.

There are eight recorded cases of 46XY sex reversed females with deletions of the short arm of chromosome 9. The breakpoints on chromosome 9 spread from p21 to p24 suggesting that the 9p24 region is involved in the differentiation of male phenotype. The patients have normal female or ambiguous external genitalia and varying grades of mixed gonadal dysgenesis. This implies that their sexual development has been perturbed during testes formation. We have collected five such patients and mapped the extent of their deletions by typing highly polymorphic microsatellite markers from the 9p23–p24 region. Loss of heterozygosity has been scored as a potential deletion of one allele. These genetic data combined with radiation hybrid mapping data for the same loci locate the smallest deletion from D9S1779, the most telomeric marker tested, to D9S1810. The estimated physical size is 8–10 Mb. We are currently testing a panel of XY females with no detectable chromosomal rearrangements for the presence of microdeletions in the identified sex reversal critical region.

Physical mapping of a candidate tumour suppressor locus for bladder cancer at 9q33. T. HABUCHI and M. KNOWLES. *Molecular Genetics Laboratory, Marie Curie Research Institute, UK*.

Detailed loss of heterozygosity (LOH) studies have indicated that there are multiple tumour suppressor loci for bladder cancer on chromosome 9q in addition to the locus at 9p21. We have previously shown that there are at least two commonly deleted regions.

In order to identify the bladder tumour suppressor genes on 9q, we have further extended our LOH studies using microsatellite markers on chromosome 9q. By analysing more than 200 transitional cell carcinomas of the bladder and upper urinary tract, we found a localised deleted region at 9q33 in 5 bladder cancers. Preliminary data indicate that the deleted region in these tumours was near to D9S195 and retention of heterozygosity was observed at other markers including D9S275, D9S258, GSN, and D9S103 at 9q33. We have constructed a YAC contig map of the region. Although published data have placed both D9S195 and D9S258 1 cM distal to D9S275, the order of these 5 markers was not defined clearly. Our physical mapping data indicate that the order is (centromere)–D9S103–D9S258–D9S195–D9S275–GSN–(telomere).

A meiotic breakpoint map near the FRDA region of chromosome 9. J. L. HAINES, K. BURGESS and H. TERWEDOW. Molecular Neurogenetics Unit, Massachusetts General Hospital, Charlestown, MA 02129.

The Human Genome Initiative has generated tremendous resources for mapping chromosome 9. Over 12000 polymorphic microsatellite markers have been generated, with hundreds of markers on chromosome 9 alone. Although excellent genetic maps using these markers have been developed, they suffer from several difficulties. These include using only a small subset of the CEPH families for the mapping, and lack of integration of markers from different groups into a single map. As part of a large collaborative effort to ease such integration and improve the resolution of the genetic markers, a strategy of using meiotic breakpoint mapping has been applied to markers in the pericentromeric region of 9q. An updated map will be presented.

Physical mapping of human RPS6 genomic locus on 9p22·3–9p23. R. ILISSON, I. PATA and A. METSPALU. Institute of Molecular and Cell Biology, University of Tartu, Tartu EE2400, Estonia.

Ribosomal protein S6 (RPS6) is unique in mammalian 40S subunits in undergoing multiple serine phosphorylation in response to various effectors and to mitogenic stimulation and thus may be implicated in cell growth control. There are several pieces of evidence that RPS6 is implicated in tumor suppression in *Drosophila* by some as yet unidentified mechanism. RPS6 gene was initially mapped by FISH to 9p21 – a chromosome region frequently deleted or rearranged in various human cancers. Therefore we started studies to analize the genomic region locus of RPS6 gene, together with functional analyses of S6. The 2·5 Mbp YAC contig was assembled using CEPH YAC clones (804 b9, 877c3, 924 c7, 936 a3), and RPS6 as well as polymorphic markers D9S162 and D9S1684, were localised within this contig. This work indicated that RPS6 lies in 9p22·3–9p23, telomeric to the IFN gene cluster. RPS6 is transcribed in a telomeric direction. We have begun to construct the a cosmid contig for RPS6. A subset of 180 clones from Lawrence Livermore chromosome 9 specific cosmid

library (obtained from University College London, Dr. Joseph Nahmias) was selected by sequence-independently amplified YAC 804-b9 from CEPH Mega-YAC library. Selected cosmid clones are further mapped into bins by EcoRI digest and the construction of contig covering about 1 Mbp region around RPS6 gene is in progress. The cosmid contig provides us with the tool for arranging ordering transcripts originated by cDNA selection.

Physical mapping, sts generation and gene isolation and analysis of chromosome 9q34. A. KUMAR², N. RAO², S. NEWEY¹, P. XU¹, J. PUFKY, H. QIU¹, R. KANDT², M. PETTENATI², R. HODGES², V. GUY¹, A. D. ROSES¹, M. A. PERICAK-VANCE¹ and J. R. GILBERT¹. Division of Neurology, Department of Medicine, Duke University Medical Center, Durham, NC, USA; Bowman Gray School of Medicine, Winston-Salem, NC, USA.

A major research effort in our laboratory is directed toward the physical mapping and isolation of genes between the DBH and D9S114 markers on human chromosome 9q34. Our primary aim is to construct a physical map in the form of both a pulse-field restriction enzyme map and a contig consisting of genomic cosmid, P1, PAC and BAC clones. Genes are being isolated utilizing these genomic clones and mapped back to the genomic contig to create a transcription map of this region.

To date we have created two contigs that contain approximately 555 kb of DNA. Contig 1 extends from roughly 40 kb proximal to DBH to about 180 kb distal to D9S66. Contig 2 contains 120–125 kb and encompasses D9S114. Based on pulsed-field mapping less than 50 kb separate the two contigs. The contigs consist of less 11 P1, 4 PAC, 1 BAC and 6 cosmid clones and 27 new STS. During the generation of these contigs some FISH confirmed P1, PAC and BAC clones were isolated which had substantial deletions, indicating that genomic fragments derived from this region may be unstable in these cloning systems.

To generate a transcription map of this region we have begun the isolation and analysis of genes located between DBH and D9S10. Utilizing a genomic fragment of approximately 108kb lying distal to DBH and proximal to D9S10, we have isolated three distinct cDNA's. Two cDNA's have been mapped back to 9q34 by FISH analysis while mapping of the third clone was inconclusive due to repeats contained within the cDNA. PCR and sequencing analysis indicate that all three cDNA's (approximate length 2·9 kb, 2·2 kb and 2·1 kb) are likely to have derived from this region. Sequencing of these partial cDNA transcripts has demonstrated different 3' UTR sequences and no strong homology with known genes. Isolation of full length clones and detailed mapping of cDNA's to the genomic clones are underway.

A dense STR map of 1.5 Mb of 9q34: small reduction in the TSC1 critical region. D. J. KWIATKOWSKI¹, D. HUMPHREY¹, M. Van SLEGTENHORST², J. ATTWOOD³, J. L. HAINES⁴, M. W. BURLEY³, N. HORNIGOLD³, M. SMITH⁵, J. NAHMIAS³, S. FAURE⁶ and S. POVEY³. ¹Harvard MS, BWH, Boston; ²Dept Clin Genet, Erasmus U, Rotterdam; ³The Galton Laboratory, UCL, London; ⁴Mol Neurogenet, Harvard MSMGH, Boston; ⁵Dept Pediatrics, UC, Irvine; ⁶Genethon, Evry.

The current critical region for the TSC1 gene is D9S149–D9S114. In concert with efforts to generate a contig of this region, we have identified 15 STR markers from this 1·5 Mb interval, and used these markers in analysis of both Venezuelan (Venz) and CEPH reference pedigrees to create

a dense genetic linkage map of the region. Six of these markers are new (those with S#s > 1000); all six have heterozygosity > 0·7. The S149–S114 interval has distance 4·3 cM (male 6·6 cM, female 3·0 cM) in the Venz, and 3·8 cM (male 3·6 cM, female 4·0 cM) in the CEPH. Meiotic mapping permits determination of the following order: S149–(S2127, S2126)–S1830–S1199–(S1198, ABO, S164)–S1793–S150–DBH–S122–S66–S114, which is consistent with that predicted by contig construction. There are two hot-spots for recombination in this region, the S1199–S1198 and S1793–S114 intervals, where the cM/Mb ratios are 6 and 4, respectively.

Application of these markers to previously described families segregating TSC, has resulted in a small reduction in the TSC1 critical region, to the S2127–S114 interval. Analysis of a 4 generation family, with lod score of 2·0 with 9q34 markers, indicates that an affected individual shows recombination with both S149 and S2127, but not other markers described here

An EST and STS-based YAC contig map of human chromosome 9q22·3. N. J. LENCH, E. A. TELFORD and A. F. MARKHAM. Molecular Medicine Unit, University of Leeds, Clinical Sciences Building, St. James's University Hospital, Leeds LS9 7TF, West Yorkshire, UK.

We have assembled a yeast artificial chromosome clone contig of the region of human chromosome 9q22·3 encompassed by the markers cen-D9S197-D9S173-tel. This contig contains 48 clones spanning approximately 4cM/27cRads. As a first step towards completing the detailed transcription map of the interval, we have mapped 8 gene sequences and 10 expressed sequence tags (ESTs). Sequence analysis and expression profiles of 7 of these ESTs is partially complete. 16 polymorphic microsatellite repeat markers (STRs) and 16 novel sequence-tagged sites (STSs) from the region are also described. The mapping of polymorphic simple tandem repeat markers has permitted the integration of existing genetic and physical maps of the region. Together these maps provide a valuable resource for fine structure mapping and DNA sequencing across the region as well as the identification of disease gene loci and the isolation of novel coding sequences.

Towards a transcriptional map of chromosome 9p13-21. M. LYNCH, A. RUIZ, S. PUIG, M. PRITCHARD and X. ESTIVILL. *Molecular Genetics Dept.*, *IRO*, *Hospital Duran i Reynals*, *Barcelona*.

As a consequence of our interest in cutaneous malignant melanoma and our findings indicating that a region of chromosome 9, centromeric to CDKN2A, is involved in the development of melanoma tumours, we are isolating transcribed sequences from the 9p13–21 region. We have 5 overlapping YACs (465 E12, 922 G2, 929 G12, 942 F10, 942 H5) which span approximately 3·5–4·0 Mb of this region from which we have constructed cosmid libraries. Some 200–250 cosmids have been picked at random from these libraries by their hybridisation to total human DNA. We have used three different strategies to identify genes within the YACs and cosmids. Firstly, we have amplified putative exons by Alu/splice PCR using the YAC DNA as a template. Secondly, 12 cosmids have been used to perform exon-trapping. Thirdly, 186 cosmids have been used to select cDNAs from foetal brain, liver, and adult muscle cDNA libraries by hybridisation (cDNA selection). Various clones are being characterized and their positions on the chromosome are being determined.

One gene already known in the region (TEK) has been re-isolated, as well as some ESTs (X85688, X85689) already in the databases. New sequences are being compared to the databases to provide clues to possible functions.

Fine mapping of the nail-patella syndrome locus and integration of new markers into the 9q34 map. I. McINTOSH^{1,2}, M. V. CLOUGH^{1,2}, A. A. SCHÄFFER³, C. A. FRANCOMANO² and M. K. McCORMICK⁴. ¹ Center for Medical Genetics and Department of Medicine, Johns Hopkins University School of Medicine, Baltimore, MD 21287. ² Medical Genetics Branch and ³ Laboratory of Genetic Disease Research, National Center for Human Genome Research, National Institutes of Health, Bethesda, MD 20892. ⁴ Molecular Neurogenetics Unit, Massachusetts General Hospital, Charlestown, MA 02129.

Nail-patella syndrome (NPS), or onychoosteodysplasia, is an autosomal dominant, pleiotropic disorder characterized by nail dysplasia, absent or hypoplastic patellae, iliac horns and nephropathy. Previous studies have demonstrated linkage of the nail-patella locus to the ABO and adenylate kinase loci on human chromosome 9q34. As a first step toward isolating the NPS gene, we present linkage analysis with thirteen polymorphic markers in five families with a total of 69 affected persons. Two-point linkage analysis with the program MLINK showed tight linkage of NPS and the anonymous markers D9S112 (LOD = 27.0, $\theta = 0.00$) and D9S315 (LOD = 22.0, $\theta = 0.00$). Informative recombination events place the NPS locus within a 1–2 cM interval between D9S60 and the adenylate kinase gene (AK1).

Three families exhibiting informative recombination events were analysed further using the latest Généthon markers [1] to (a) reduce the candidate region, and (b) integrate these markers into the existing map. Two point linkage analyses gave LOD scores of $12\cdot6$ and $11\cdot5$ ($\theta=0\cdot00$) for D9S1798 and D9S1821, respectively, and both can be placed within the D9S60-AK1 interval. Furthermore, D9S1789, D9S1825 and D9S1840 also showed no recombination with NPS but were uninformative relative to D9S60. D9S1113 and D9S1829 mapped centromeric of NPS but cannot be positioned relative to D9S60. D9S1827 could be positioned telomeric of SPTAN1 (figure). Physical mapping places D9S1798 in the same contig as D9S315 and D9S1144 within a contig containing AK1. STS-mapping of CEPH YACs [2] around D9S60 suggests the order shown in the figure (top right). D9S1113 is therefore marks the centromeric boundary of the NPS candidate region and PBX3 is excluded as a candidate gene. Two other potential candidate genes have been mapped to 9q34 and have not been excluded from the D9S60-AK1 interval: a receptor involved in the regulation of collagen expression (TGFBR1) and a zinc finger-containing transcription factor (ZNF79). Mapping of these loci relative to the NPS candidate region is in progress.

- [1] C. Dib et al. (1996) Nature **380**, 152–4.
- [2] T. J. Hudson et al. (1995) Science **270**, 1945–54.
- [3] C. L. Shovlin et al. (1995) Ann. Hum. Genet. **59**, 381–2.

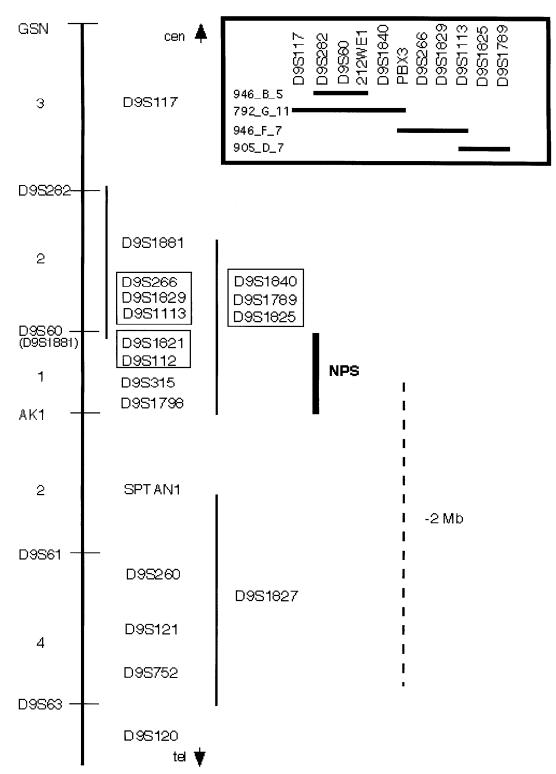


Fig. 1. Loci to the left of the line are ordered as described [3] with distances as shown (cM). The order of markers to the right of the line was determined during the course of this work or from refs [1] & [2]. Defined genetic distances [1]: D9S1881–0·5 cM–D9S1789/D9S1825; D9S266–0·9 cM–D9S1821–3·5 cM–D9S260. Loci which could not be ordered definitively are boxed. Ambiguity lines indicate the range of possible positions where crucial meioses were uninformative. The vertical bar indicates the NPS candidate region. The box in the top right of the figure shows the results of STS mapping of markets around D9S60 using CEPH YACs [2].

A sequence ready contig spanning the TSC1 candidate interval on chromosome 9. J. NAHMIAS¹, N. HORNIGOLD¹, M. van SLEGTENHORST², C. HERMANS², J. YOUNG¹, R. EKONG¹, S. ROUSSEAUX¹, M. FOX¹, D. KWIATKOWSKI³, J. ATTWOOD¹, M. SMITH⁴, X-N. CHEN⁵, J. R. KORENBERG⁵, S. POVEY¹ and J. WOLFE¹. ¹ The Galton Laboratory, University College London, 4, Stephenson Way, London NW1 2HE, UK; ² Department of Clinical Genetics, Dr. Molewaterplein 50, NL-3015 GE Rotterdam The Netherlands; ³ Harvard Medical School, Brigham and Women's Hospital, Longwood Medical Research Center, 221, Longwood Avenue, Boston, MA 02115 USA; ⁴ University of California at Irvine, Dept of Paediatrics/Human Genetics, Medical Sciences I, C-234 Irvine CA 92717 USA; ⁵ Cedars-Sinai Research Institute, UCLA, Medical Genetics Dept., 110 George Burns Road, Davis Building, Suite 2069, Los Angeles, CA 90048–1869 USA

The genetic disease tuberous sclerosis is caused by mutation in one of two genes, TSC1 and TSC2 mapping to 9q34 and 16p13 respectively. While TSC2 has been cloned, TSC1 has only been assigned to the 4 cM interval between D9S149 and D9S114 and within this interval contradictory data have been described which have made it impossible to narrow the interval any further. We have decided to clone the entire region as a basis from which to identify candidate loci. We have previously published a step on this path, (J. Nahmias et al. (1995). Eur. J. Hum. Genet. 3, 65–77, van Slegtenhorst et al. (1995). Eur. J. Hum. Genet. 3, 78–86) and by a combination of techniques and by screening several different libraries, we have now been able to assemble an almost continuous cosmid, BAC and PAC contig extending over 1·8 Mb with one gap (estimated at 20 kb by FISH to extended DNA). This contig includes the entire candidate region, its average depth is about 8 clones and its minimum depth is 2 clones. The contig includes 17 polymorphic loci which have been accurately placed and several known genes including CEL, ABO, SURF@, DBH, and VAV2. We have been actively mapping ESTs, trapped exons (and their derived cDNAs) and cDNAs obtained by cDNA selection most of which have provided new STSs. We estimate that we have identified, on average, one polymorphic locus and two to three transcription units per 100 kb across the interval.

Linkage studies of Walker-Warburg Syndrome (WWS) and chromosome 9q31–32. HOPE NORTHRUP¹, ESTANISLADO RODRIGUEZ Jr.¹, KIT-SING AU¹, SUSAN BLANTON², and WILLIAM B. DOBYNS³. ¹Department of Pediatrics, The University of Texas Medical School – Houston, Texas; ²Department of Pediatrics, University of Virginia, Charlottesville, Virginia; ³Departments of Neurology and Pediatrics, University of Minnesota Medical School, Minneapolis, Minnesota.

The gene responsible for Fukuyama congenital muscular dystrophy (FCMD) has been assigned to chromosome 9q31–32 by homozygosity mapping. We tested several markers for this region for linkage in patients with Walker-Warburg syndrome (WWS).

Cobblestone lissencephaly (CL) is the brain malformation observed in several related syndromes. It consists of lissencephaly or polymicrogyria with a pebbled surface, white matter changes, enlarged ventricles, cerebellar malformation and brainstem hypoplasia. FCMD consists of mild CL and congenital muscular dystrophy. Walker-Warburg (WWS) and muscle-eye-brain (MEB) syndromes both consist of more severe CL, retinal changes and congenital muscular dystrophy. Inheritance of the same 9q31–32 alleles was demonstrated in two Japanese sibs with FCMD and WWS, which suggests that these disorders may be allelic although the older sib probably had MEB and not FCMD.

We tested several markers from the 9q31–32 region linked to FCMD to determine whether FCMD and WWS are allelic disorders. Our study included seven families (six consanguineous) with one or

more children affected with WWS. The loci tested included D9S127, D9S306 and D9S59, which are known to flank the FCMD locus. Three families, while unable to exclude linkage to WWS, were not consistent with linkage of WWS to this region. The other four families yield small positive LOD scores and thus cannot be excluded from linkage to the FCMD locus.

Physical mapping and sequence analysis in the tumor suppressor locus on 9p. O. I. OLOPADE, H. POMYKALA, L. SVEEN, W. STADLER, F. HAGOS, C. WALKER, H. ARADDANN, DENISE BURIAN and BENSON ROE. Section of Hematology/Oncology, Dept of Medicine, University of Chicago, IL 60637. The University of Texas MD Anderson Cancer Center, Smithville, Texas. University of Oklahoma.

One of the most common recurring genetic abnormalities in cancer cells is homozygous loss of DNA sequences on the short arm of chromosome 9. We previously reported the assembly of a 2·8 MegaYac contig on 9p21 encompassing the CDKN2, CDKN2B, MTAP and IFN genes. CDKN2 has been identified as the tumor suppressor gene in this locus but several questions remain about the contribution of other genes and the complexity of this locus. To have a better understanding of of the structural organization of this cluster of genes and to search for additional coding regions, we have assembled more than 100 overlapping cosmids on 9p21 and completely sequenced 2 overlapping cosmids containing CDKN2 and CDKN2B. A preliminary database search revealed no new genes within the two cosmids. However, several deletion breakpoints in tumor cells cluster within the cosmids. Further analysis of the sequences at the breakpoint juncture may shed light on the chromosomal mechanism of the deletions.

We have also characterized the genomic organization of the MTAP gene. MTAP maps approximately 100 kb telomeric to CDKN2 and both genes are often co-deleted in multiple tumor types. Two major transcripts of 2·5 kb and 7·5 kb are identified for MTAP, which is constitutively expressed in all tissues but absent from human cancer cell lines with homozygous deletion on 9p21. MTAP spans approximately 20 kb, divided into 8 exons and 7 introns. Several deletion breakpoints in tumor cells have been mapped within the gene which suggests that the normal regulation of this gene may also be disrupted by chromosomal deletions involving the neighbouring CDKN2 gene. MTAP has been highly evolutionarily conserved and maps to rat chromosome 5 in the region of synteny to human chromosome 9. Rat mtap is homozygously co-deleted with CDKN2 in rat renal cell cancers.

Use of meiotic breakpoint panel to map markers into the interval between D9S60 and ABL. L. OZELIUS¹, J. ATTWOOD², M. REBELLO², S. POVEY², and X. BREAKEFIELD¹. ¹Molecular Neurogenetics Laboratory, Massachusetts General Hospital, Charlestown, Ma. 02129, USA; ²MRC Human Biochemical Genetics Unit, UCL, Wolfson House, 4 Stephenson Way, NW1 2HE, UK.

Several new genetic linkage maps exist for chromosome 9. Each has been developed by a different group using their own simple sequence repeat polymophism (SSRP) markers with data generated on a small subset of CEPH families. For these reasons, it has been very difficult to relate these markers to each other, integrate them into the previously developed maps and assign them to regions

containing disease genes. The use of the recently developed meiotic breakpoint panel should circumvent the need to genotype the remaining 30–35 CEPH families with all of these new markers. Instead, with the identification of recombinants in a particular region of interest, only the recombinant individual and their relevant relatives (usually 5 individuals total) need be typed with the new markers assigned to that interval. If the markers are informative in the recombinant families, then this represents a fast and effective strategy for integrating these genetic maps. We are interested in the breakpoint interval between D9S60 and ABL, containing the markers D9S60-D9S260-D9S290-D9S159-D9S65-ABL, because this region also cotains the DYT1 gene. Thus far, we have tested seven markers in this interval including two new SSRPs from cosmids containing the AK1 and SPTAN1 genes. Another 15–20 markers that have been roughly placed in the region between D9S60-ABL and will be mapped. Hopefully, using this method, we can begin to generate an integrated genetic map for this interval including most of the available markers.

A meiotic breakpoint map of the gsn region of chromosome 9. M. A. PERICAK-VANCE, M. EPSTEIN, J. SARRICA, J. RIMMLER and M. MENOLD. Division of Neurology, Duke University Medical Center, Durham, NC 27710.

The Human Genome Initiative has provided the resources for generating thousands of markers dispersed throughout the genome. Several hundred of these are localized to chromosome 9. While several excellent genetic maps of chromosome 9 exist they are not comprehensive. There are many markers that are potentially useful in disease mapping that are only regionally located or are at best localized in a small subset of the CEPH families. Another problem is the lack of integration of the various available maps. As part of a large collaborative effort undertaken by the chromosome 9 community, we are using the approach of meiotic breakpoint mapping in an effort to produce a better integrated and more comprehensive map of the chromosome.

The data included in this abstract involves the GSN region on chromosome 9 between the markers D9S131 and D9S60. Specifically we will attempt to fine map the regionally localized tetranucleotide repeat markers, D9S762, D9S250, D9S778, D9S779, D9S774 between the identified breakpoints in this region. Additional markers will be included as needed. An updated map will be presented.

Genetic and physical mapping in the distal portion of chromosome 9p – toward a more detailed and reliable map of the region. M. REBELLO¹, J. ATTWOOD¹, R. EKONG¹, M. FOX¹, S. ROUSSEAUX¹, S. FAURE², S. POVEY¹. ¹MRC Human Biochemical Genetics Unit, UCL, London; ²Genethon, 1 rue de l'International, Paris.

The genetic map of 9p24 has been enhanced by adding in the Genethon markers (Nature 380:1996) not previously included. The new map has then been further refined by retyping STSs on a number of individuals causing apparent double recombinants in the genetic map. Where repeated typing of individuals has not resolved these conflicts, re-evaluation of the map order has been carried out to reduce the number of cross-overs per chromosome. This work has helped generate a new order for the markers in distal 9p:- pter, (D9S1779, D9S1858), D9S129, D9S143, D9S54, (D9S1813, D9S1871, D9S288, D9S1873, D9S178, D9S1792, D9S1810), (D9S132, D9S199), D9S25, (D9S1686, D9S324,

D9S281, D9S1852), (D9S1676, L256, D9S286), D9S1681, D9S144, D9S168, (D9S256, D9S269), (D9S268, D9S267, D9S1808), D9S1687, (D9S1869, D9S274), D9S285, (D9S1839, D9S156, D9S1782), D9S157, (D9S162, D9S1684, D9S33, D9S1778), (D9S1814, D9S1846, @IFN, D9S1870), D9S126, D9S741.Markers in parentheses cannot be separated.

The genetic map has been used to construct a meiotic breakpoint map of 9p and this, as well as the full genetic map of chromosome 9p, will be presented.

The physical map of 9p has been improved by FISH mapping cosmids for STSs on three translocation cell lines, DD1151, HHW1069 and DD0118. This work supports the marker order on the genetic map and has also added information about the orientation of the two most distal markers, D9S1779 and D9S1858, with D9S1779 being distal to D9S1858. We have also shown that a cosmid positive for the EST D9S989E maps distal to D9S1858, confirming the presence of expressed genes in this very distal region.

Physical mapping of 9p13 using BACS and radiation hybrids. M. RIDANPÄĹ, P. KIVIPENSAS¹, T. PARKKINEN¹, N. LAING², and I. KAITILA³.¹ Department of Medical Genetics, University of Helsinki, Finland; ²Australian Neuromuscular Research Institute, University of Western Australia; ³Department of Clinical Genetics, Helsinki University Hospital, Finland.

Cartilage-hair hypoplasia is an autosomal recessive form of chondrodysplasia presenting with short stature, hair hypoplasia, hypoplastic anemia, and defective cell-mediated immunity. Based on the pleiotropic expression the gene for cartilage-hair hypoplasia (CHH) should code for an important factor in cellular proliferation and/or differentiation. The previous linkage and linkage disequilibrium mapping results localize CHH approximately 0·3 cM on the proximal side of the microsatellite marker D9S163. To further characterize this region we are doing radiation hybrid mapping and construction of a physical map using bacterial artificial chromosomes (BACs) and P1s. However, the contig is not ready to be sequenced.

Radiation hybrid mapping with the Medium Resolution Standard G3 Hybrid Panel has allowed us to refine the localization of GALT and CNTFR in the region between D9S165 and D9S163. Furthermore, both TPM2 and PAX5 were localized between markers D9S163 and D9S50. Interleukin-11 receptor alpha-chain gene (IL11RA) and a cDNA called HA2337 (protein kinase close to D9S163) were excluded as possible candidate genes for CHH by localizing them on the proximal side of the CHH region. During construction of the BAC/P1 contig, radiation hybrid mapping has helped us in orientation and estimation of the physical distances. We also report a new, polymorphic CA repeat (6 alleles detected in a Finnish population) in the near vicinity of D9S163.

Cytogenetic characterization of 9p rearrangements in breast cancer cell lines. LARISSA SAVELYEVA, ANDREAS CLAAS and MANFRED SCHWAB. German Cancer Research Center, Heidelberg, Germany

The evaluation of the G-banding karyotypes and *in situ* hybridization with a total chromosome 9 library of 15 female breast cancer cell lines revealed significant frequency of structural alterations of 9p.To define in more detail alterations involving 9p we have used FISH with CEPH-Mega YAC

clones. To confirm available mapping data we performed cytogenetic mapping by dual-colour FISH of 30 YACs, previously assigned to the short arm of chromosome 9 in normal human lymphocytes. Using the non-chimeric probes for detection of chromosome alterations, we identified heterozygous and homozygous deletions of chromosome 9p in 9/15 breast cancer cell lines. 9p was deleted to various extents, including large deletions involving most of the chromosome arm and small deletions spanning only the region distal to marker FB2G7. In addition, translocations, inversion and insertion affecting distal 9p were observed in three other cell lines. A region bordered by cosmid 43G11 (positive for D9S1858) and YAC 727D12 (most distal positive marker D9S178, most proximal positive marker FB2G7) has been identified as smallest region of chromosomal instability shared by 9 different cell lines. The genetic distance between these markers cannot be resolved. Only radiation hybrid mapping reveals a distance of maximal 15 cR.

The precise mapping of the breakpoints will allow us to define the critical region, which can contribute to breast cancer tumorigenesis.

Chromosome breakage hotspots in 9p and delineation of the critical region for the 9p deletion syndrome. S. SCHWARTZ, C. A. CROWE¹, J. M. CONROY, J. M. HAREN, M. A. MICALE and L. A. BECKER. Center for Human Genetics, Department of Genetics, Case Western Reserve University and University Hospitals of Cleveland, and ¹MetroHealth Medical Center, Cleveland, Ohio.

The 9p deletion syndrome is a well characterized syndrome which includes: dysmorphic facial features (trigonocephaly, midface hypoplasia, upward slanting palpebral fissures and a long philtrum) and mental retardation. Although over 90 patients have been identified and studied with standard cytogenetic analysis, limited molecular studies have been undertaken. The majority of these patients appear to have similar breakpoints in 9p22, but some cases show phenotypic heterogeneity. In order to more precisely define the breakpoints of the deleted chromosomes, we have studied 26 patients with a presumptive diagnosis of deletion 9p syndrome with high resolution cytogenetics, FISH using over 40 YACs, and PCR with 25 different STSs.

Results from this study have provided insight into the mechanisms of breakage leading to the deletion and resultant phenotype-karyotype correlations: (1) Seven different breakpoints have been localized to a region in 9p22/p23 between D9S274 and D9S162. Each of these breakpoints have been localized to a specific YAC within this region. (2) Nine of the patients were determined to have the same breakpoint within this region, localized between D9S274 (948-h-1) and D9S285 (767-f-2). The large number of breaks at the same location suggests the existence of a chromosome breakage hotspot and a possible repeat sequence involved in the formation of this deletion. (3) Eleven patients were found to have five different breakpoints within an approximate 2 Mb region of DNA in 9p22. The breaks were clustered between D9S1709 and D9S162 and were suggestive of a breakpoint cluster region because of the frequency and number of breaks. It is very likely that this region is comprised of repeated sequences that may predispose this area to misalignment and/or exchanges during pairing in meiosis. (4) Clinical evaluation of our patients revealed that the majority of the patients had classical features of 9p deletion syndrome, but that some were without the major features of the syndrome. Based on the molecular studies of these patients, and previously reported studies, we have refined the localization of the putative critical region for the 9p deletion syndrome to a region in 9p23from D9S286 to D9S267.

Saturation of the genetic map and expansion of the physical map surrounding the familial dysautonomia gene on human chromosome 9. S. A. SLAUGENHAUPT¹, D. MOODY¹, C. B. LIEBERT¹, S. POVEY², M. REBELLO², J. ATTWOOD² and J. F. GUSELLA¹. ¹Molecular Neurogenetics Unit, Massachusetts General Hospital, Charlestown, Massachusetts, 02129, USA; MRC Human Biochemical Genetics Unit, UCL, Wolfson House, 4 Stephenson Way, London, NW1 2HE, UK.

Genotyping of the CEPH reference pedigree panel with a large number of markers on human chromosome 9 has permitted the construction of a panel of breakpoints that define specific recombination intervals. Therefore, new markers that have been regionally localized can be rapidly added to the linkage map by genotyping only a few informative individuals. The breakpoint map surrounding the familial dysautonomia gene (DYS) spans 9q22·3–q31 and includes the following markers: D9S127–D9S53–D9S172–D9S261/D9S748–D9S58–D9S160–D9S131–D9S279–D9S289. A recent scan of the published databases suggests that an additional 25 markers may map within this small segment of the chromosome. We have added 20 new markers to the breakpoint map: 9 mapped to a specific interval, 4 were regionally localized, and 7 were added by physical mapping. An updated genetic map will be presented.

We have also continued to expand and saturate the physical map surrounding D9S58 in our efforts to clone the familial dysautonomia gene. We currently have a YAC contig that spans > 1·3 Mb and a sequence ready cosmid contig that spans > 800 kb. In addition, we have isolated and ordered BAC clones that cover the entire candidate region to make the area more amenable to direct sequencing. A recombination event has been identified in a new family that defines D9S58 as a distal flanking marker and places the gene between D9S58 and D9S748. This candidate region can be further narrowed to the interval between D9S261 and D9S310 using linkage disequilibrium. An updated physical map of the DYS region in distal 9q31 will be presented.

Analysis of the VAV2 and bromodomain homeotic gene region on chromosome 9q34·3. M. SMITH, K. HANDA. Dept. of Pediatrics, University of California, Irvine CA.

We have analyzed the genomic structure of the Vav2 gene region and have determined that Vav2 extends over 150 kb on chromosome 9q34·3. We have detected Vav2 exonic sequences in cosmids 152F5, 272C1, 79B4 and 7A10 (provided to us by Dr. Janssen). Vav2 sequences were also mapped within the plasmid MCT136 (ATCC) and in cosmid 17BE (provided to us by Drs Woodward, Nahmias and Povey). Our results indicate that there are at least two copies of Vav2 on chromosome 9q34·3 and that they extend from cosmid 152F5 (proximal) to cosmid 17BE (distal). The 3 prime ends of the Vav2 genes are positioned toward the centromere and the 5 prime ends are positioned toward the telomere. The dinucleotide repeat polymorphic marker D9S122 is located in 152F5. We have determined that the cosmid 17BE and the cosmid 82C2 (provided to us by Drs Murrell and Buckler) contain sequence with a high degree of homology (6·2e-13) to an anonymous marker in Genbank designated D26362. D26362 encodes duplicated bromodomain regions. It is highly homologous (homology score 6·0e-174) to the Ring3 gene which is the human homolog of the Drosophila female sterile homeotic gene which is required for proper functioning of homeotic genes. The 5' end of the bromodomain homeotic gene on chromosome 9q34:3 lies toward the centromere and the direction of transcription is therefore opposite to that of the Vav2 gene. Our findings indicate that there are most likely two highly homologous but non-identical copies of the bromodomain homeotic gene in the 9q34·3 region, one contained partly within cosmid 17BE and the other

contained within cosmid 82C2. These two cosmids apparently do not overlap. We have identified a polymorphic marker P6 which maps within cosmid 82C2. P6 contains 500 bp representing the most 3' sequence in D26362 (the bromodomain homeotic gene). The polymorphic marker A6, recently reported by Au et al. J. Med. Genet. 33, 559 1996, maps within the cosmid 82C2.

Terminal deletions of distal 9p define a minimum region associated with male to female sex reversal. R. VEITIA¹, M. NUNES¹, R. BRAUNER², O. JOANNY-FLINOIS³, M. FELLOUS¹ and K. McELREAVEY¹. ¹Unit- d'Immunog-n-tique Humaine, Institut Pasteur, Paris; ²Unit-d'Endocrinologie et Croissance, Hôpital Necker-Enfants Malades, Paris; ³Centre Hospitalier de Charleville-M-zi-res.

Monosomy of distal 9p is frequently associated with abnormal development of external genitalia in 46,XY boys. In 6 of these cases the individual was given female gender assignment. Alignment of the deleted portions indicates that the minimum region associated with male to female sex reversal is 9p24-pter. We describe two cases of 46,XY females partially monosomic for 9p. Patient A has a 46,XY karyotype with an inverted duplication of 9p involving 9p12 to 9p23 associated with a loss of 9p24-pter and patient B has a mosaic karyotype: 46,XY, t(9;14)(p23;q12), -der(14)t(9;14), +r(14) / 45,XY, t(9;14)(p23;q12),-der(14)t(9;14). Definition of the breakpoint using somatic cell hybrids containing only the rearranged 9p indicated that in patient A the breakpoint was located between markers D9S256 and D9S144 and in patient B the breakpoint was delimited between markers D9S144 and D9S168. In both cases this corresponds to the position 9p23·3-9p24·1. The transcription factor NF1B which was previously mapped to 9p24·1 by in situ hybridisation was located proximal to both breakpoints. Microsatellite analysis using highly polymorphic 9p markers demonstrated a paternal origin of the rearranged chromosome 9 in both patients. These studies define the minimum region associated with male to female sex reversal as 9p24·1-pter.